THE JOURNAL OF BIOLOGICAL CHEMISTRY VOL. 286, NO. 26, pp. 23063–23076, July 1, 2011
© 2011 by The American Society for Biochemistry and Molecular Biology, Inc. Printed in the U.S.A.

Characterization of Prefibrillar Tau Oligomers *in Vitro* and in Alzheimer Disease*[S]

Received for publication, March 8, 2011, and in revised form, May 4, 2011 Published, JBC Papers in Press, May 6, 2011, DOI 10.1074/jbc.M111.237974

Kristina R. Patterson[‡1], Christine Remmers[‡], Yifan Fu[‡], Sarah Brooker[‡], Nicholas M. Kanaan[§], Laurel Vana[‡], Sarah Ward[‡], Juan F. Reyes[‡], Keith Philibert[¶], Marc J. Glucksman[¶], and Lester I. Binder[‡]

From the [‡]Department of Cell and Molecular Biology, Feinberg School of Medicine, Northwestern University, Chicago, Illinois 60611, the [§]Division of Translational Science and Molecular Medicine, Michigan State University, Grand Rapids, Michigan 49503, and the [¶]Midwest Proteome Center and Department of Biochemistry and Molecular Biology, Rosalind Franklin University of Medicine and Science/Chicago Medical School, Chicago, Illinois 60064

Neurofibrillary tangles, composed of insoluble aggregates of the microtubule-associated protein Tau, are a pathological hallmark of Alzheimer disease (AD) and other tauopathies. However, recent evidence indicates that neuronal dysfunction precedes the formation of these insoluble fibrillar deposits, suggesting that earlier prefibrillar Tau aggregates may be neurotoxic. To determine the composition of these aggregates, we have employed a photochemical cross-linking technique to examine intermolecular interactions of full-length Tau *in vitro*. Using this method, we demonstrate that dimerization is an early event in the Tau aggregation process and that these dimers self-associate to form larger oligomeric aggregates. Moreover, using these stabilized Tau aggregates as immunogens, we generated a monoclonal antibody that selectively recognizes Tau dimers and higher order oligomeric aggregates but shows little reactivity to Tau filaments *in vitro*. Immunostaining indicates that these dimers/oligomers are markedly elevated in AD, appearing in early pathological inclusions such as neuropil threads and pretangle neurons as well as colocalizing with other early markers of Tau pathogenesis. Taken as a whole, the work presented herein demonstrates the existence of alternative Tau aggregates that precede formation of fibrillar Tau pathologies and raises the possibility that these hierarchical oligomeric forms of Tau may contribute to neurodegeneration.

Alzheimer disease (AD)[2] is characterized by the extracellular accumulation of plaques composed of amyloid β (Aβ) and the intracellular accumulation of the microtubule-associated protein Tau into neurofibrillary tangles (NFTs). Unlike Aβ plaques, the spatial and temporal progression of NFTs positively correlates with the progression of clinical symptoms (1, 2). Additionally, Tau is necessary for Aβ-induced neurotoxicity in cell culture and transgenic mouse models (3–5). Tau inclusions are found in other tauopathies that lack Aβ pathology, including Pick's disease, corticobasal degeneration, and progressive supranuclear palsy (6). Notably, mutations in the *tau* gene cause some forms of frontotemporal dementia (7–10), signifying that Tau dysfunction is sufficient to cause neurodegeneration.

Under physiological conditions, Tau is a highly soluble microtubule-associated protein with limited secondary structure (11). In AD and other tauopathies, however, Tau becomes hyperphosphorylated and undergoes conformational shifts that lead to its self-association into filamentous and non-filamentous aggregates (12). Filamentous Tau is highly ordered, possessing β-pleated structure, as is typical of amyloidogenic proteins (13). Although NFT load correlates with neuronal cell loss and the severity of cognitive impairment in AD, whether or not these filamentous Tau aggregates are neurotoxic remains controversial. Overexpression of both wild type and mutant Tau induces neurodegeneration in various animal models (14–19); however, memory deficits and cell loss precede detectable NFT-like Tau pathology (20, 21). Moreover, suppression of Tau expression improves memory function and halts further cell loss yet NFTs persist, suggesting that neurofibrillary pathology is not sufficient for neurodegeneration (22, 23). Importantly, neurodegeneration occurs in some animal models overexpressing Tau despite the absence of overt neurofibrillary pathology (19, 24). Thus, NFTs are not required for and may not be the primary cause of neurotoxicity and cognitive dysfunction. In fact, levels of early Tau multimeric aggregates that preceded NFTs correlated with memory deficits in transgenic mice that overexpress Tau (25). Collectively, these studies strongly suggest that an intermediate Tau aggregate preceding NFT formation may be responsible for neuronal dysfunction observed in AD and other tauopathies.

Although prefibrillar Tau aggregates have been isolated from AD homogenates, the precise composition of these aggregates is unclear (26–28). Past attempts to characterize the earliest stages of Tau multimer formation *in vitro* were contingent upon disulfide bridge formation (26, 29). However, the formation of disulfide bridges can inhibit aggregation of Tau isoforms containing four microtubule binding repeats (MTBRs) (30–32), and aggregates of the four repeat isoforms are associated with many of the neurodegenerative

* This work was supported, in whole or in part, by National Institutes of Health Grants T32 AF020506 (to K. R. P.), AG09466 (to L. I. B.), National Center for Research Resources S10 RR19325 (to M. J. G.), and Health Resources and Services Administration C76 HF03610-01-00 (to M. J. G.).

[S] The on-line version of this article (available at http://www.jbc.org) contains supplemental Figs. S1–S3.

[1] To whom correspondence should be addressed: 300 E. Superior St., Tarry 8-754, Chicago, IL 60611. Tel.: 312-503-0824; Fax: 312-503-7912; E-mail: k-patterson@md.northwestern.edu.

[2] The abbreviations used are: AD, Alzheimer disease; NFT, neurofibrillary tangle; Aβ, amyloid β; MTBR, microtubule binding repeat; B4M, benzophenone-4-maleimide, AA, arachidonic acid; TR, Thiazin Red; TOC1, Tau oligomeric complex-1; SELDI-TOF, surface enhanced laser desorption and ionization time of flight.

This is an Open Access article under the CC BY license.

tauopathies (33). In this study, we describe a cross-linking technique that does not rely upon oxidative conditions. Using this method, we clearly demonstrate that Tau dimers are aggregation intermediates in the formation of higher order oligomers. Supporting the premise that Tau dimer and oligomer formation are important disease-related events, we generated a monoclonal antibody that selectively recognizes Tau dimers and higher order oligomeric aggregates. Interestingly, these oligomeric aggregates are markedly elevated in AD. Moreover, immunohistochemical studies with this antibody indicate that Tau oligomerization precedes the formation of mature NFT inclusions. Collectively, our findings demonstrate that Tau dimers and higher order oligomers form during the earliest stages of AD pathogenesis and may represent a prefibrillar toxic form of aggregated Tau.

EXPERIMENTAL PROCEDURES

Recombinant Tau Protein Expression and Purification

Tau proteins are numbered according to the largest isoform found in the central nervous system (hTau40), which consists of 441 amino acids and contains both alternatively spliced N-terminal exons and four MTBRs. HTau40 was used for all experiments except where otherwise indicated. The Tau MTBR construct consisting of residues 244–372 was generated by creating a linear PCR product of this region. An EcoRI restriction site and methionine residue were added N-terminal to residue 244 as well as a poly-His tag and NotI restriction site C-terminal to residue 372. The linear PCR product was inserted into the pET-17b vector (Novagen) via EcoRI/NotI digestion followed by T4 ligation. All other Tau constructs are cloned into vector pT7c and are described elsewhere (34–37, 86). Tau constructs were expressed in *Escherichia coli* and purified using TALON metal affinity resin (Clontech) followed by size exclusion chromatography as previously described (36, 38).

In Vitro Aggregation

Tau—Aggregation was induced with arachidonic acid (AA) as previously described (39). Briefly, Tau proteins (2–16 μM) were incubated at room temperature or at 37 °C for deletion mutants. Aggregation assays were performed in a solution containing 50 mM HEPES, pH 7.6, 50 mM KCl, and 5 mM DTT (unless otherwise indicated) in the presence of 37.5–150 μM peroxidase-free AA (Cayman Chemical). Working solutions of AA were prepared in 100% ethanol immediately prior to use.

α-Synuclein—Untagged recombinant full-length human α-synuclein was prepared and aggregated as previously described (40). Briefly, α-synuclein (4 μM) was incubated at 37 °C in 10 mM HEPES, pH 7.6, 100 mM NaCl, and 5 mM DTT in the presence of 200 μM AA for 24 h.

Aβ—Recombinant human Aβ42 (rPeptide) HFIP (1,1,1,3,3,3-hexafluoro-2-propanol)-treated stocks were prepared as previously described (41). Aβ42 oligomers and filaments were generated according to established protocols (41) with the exception that 4 mM HEPES, pH 8.0, was substituted for Ham's F-12 media. In all cases, aggregation was confirmed using transmission electron microscopy (EM). Samples were fixed with 2–10% glutaraldehyde, spotted on formvar/carbon-coated copper grids (Electron Microscopy Sciences), and stained with 2% uranyl acetate.

Benzophenone Cross-linking

HTau40 (15 μM) was reacted with a 10-fold molar excess of benzophenone-4-maleimide (B4M) cross-linker (Invitrogen) in the dark for 4 h in 100 mM Tris, pH 7.4, 0.1 mM EGTA, and 0.5 mM Tris(2-carboxyethyl)phosphine hydrochloride. The reaction was quenched with 5 mM DTT and excess B4M was removed using Nanosep centrifugal filter devices (Pall; MWCO 30 kDa). B4M-labeled Tau (8 μM) was aggregated overnight in 100 mM Tris, pH 7.4, 0.1 mM EGTA, and 5 mM DTT in the presence of AA as described above. Cross-linking was induced with shortwave UV light (254 nm) for 5 min unless otherwise indicated. For sedimentation analysis, samples were centrifuged in a TLS-55 Beckman rotor over a 40% glycerol cushion at 269,000 × *g* for 30 min at 25 °C. The supernatant was collected and the pellet was resuspended in 100 mM Tris, pH 7.4.

Electroelution

Cross-linked hTau40 aggregates were concentrated by sedimentation (as described above), diluted in Laemmli buffer, heated in a boiling water bath for 10 min, and separated by SDS-PAGE using 4–8% linear gradient polyacrylamide gels. Gels were stained with the E-Zinc Reversible Stain Kit (Thermo Scientific) according to the manufacturer's instructions. Individual bands were isolated and placed inside D-Tube Dialyzers (MWCO 6–8 kDa, Novagen). Samples were electroeluted for 5 h at 150 V in 25 mM Tris, 192 mM glycine, and 0.025% SDS. Electroeluted proteins were concentrated to ~50 μl volume with Pall Nanosep centrifugal concentrators prior to incubation in 400 μl of SDS-away (Protea Biosciences) overnight at −20 °C to precipitate the proteins. Samples were centrifuged at 18,000 × *g* for 10 min at 4 °C, the pellets were resuspended in 400 μl of SDS-away, recentrifuged, and finally resuspended in 50 mM HEPES, pH 7.6, 50 mM KCl, 0.01% Triton X-100. Samples were boiled for 5 min and centrifuged at 16,000 × *g* for 1 min to remove insoluble proteins.

Mass Spectrometry Analysis

Protein samples were subjected to analysis by surface enhanced laser desorption and ionization time of flight (SELDI-TOF) mass spectrometry to examine the distribution of masses of protein components. Samples were spotted in three successive 5-μl aliquots onto individual spots of a ProteinChip NP20 Array (Bio-Rad) and allowed to partially air dry for ~10 min to reduce the volume between applications. The chip was then washed three times with 5 μl of distilled water and air-dried prior to the addition of 2.5 μl of 10 mg/ml sinapinic acid (Bio-Rad) in 60% acetonitrile, 0.1% formic acid. Controls omitting the air drying for multiple applications of the sample as well as omitting the formic acid with matrix crystallization indicated no difference in the distribution of multimers (supplemental Fig. S2). Samples were analyzed using a Bio-Rad ProteinChip System 4000 Enterprise mass spectrometer calibrated against the Bio-Rad All-in-1-Protein Standard. Each spot was divided into 10 partitions with 210

shots/partition and the data were collected at a laser energy of 3000 joule with a mass range between 10 and 160 kDa unless otherwise indicated.

Tau Oligomeric Complex-1 (TOC1) Antibody Generation

Mouse monoclonal antibodies were raised against electro-eluted cross-linked Tau dimers. Female Tau null mice (The Jackson Laboratory; stock number 7251) were immunized subcutaneously five times with 2–10 μg of cross-linked Tau dimer. For the final two immunizations, 100 μg of cross-linked Tau oligomers (hTau40 incubated in the presence of AA for 15 min, cross-linked, and flash frozen) was administered. Once the desired serum titer was attained, splenocytes were isolated and fused to SP2/o myeloma cells (42). Two weeks after hybridoma selection in hypoxanthine/aminopterin/thymidine medium, positive clones were chosen based on their ability to bind Tau oligomers but not Tau monomer. One cell line, TOC1, was subcloned two times to ensure monoclonality and hybridoma stability. The clone was adapted to serum-free medium, grown in a CELLine CL 1000 Bioreactor (Sartorius), and the antibody purified by size exclusion chromatography prior to storage in HEPES-saline buffer, pH 7.4, containing 50% glycerol. Isotyping indicated that TOC1 was of the IgM isotype.

Human Brain Homogenates

Frozen frontal cortex samples from control (Braak I-III) and AD brains (Braak V-VI) were obtained from Rush University Medical Center or the University of Miami Medical Center. Samples were homogenized as previously described (43). For denaturing conditions, homogenates were diluted in 2× Laemmli buffer, heated in boiling water for 5 min, and briefly centrifuged at 8,000 × g for 3 min to remove cellular debris prior to collection of the supernatant. For non-denaturing conditions, homogenates were briefly centrifuged at 3,000 × g for 10 min.

Immunoblots

Recombinant Tau and human brain homogenate samples were separated by SDS-PAGE on 4–15% linear gradient gels and transferred to nitrocellulose membranes as described previously (43). For dot blots, samples were spotted directly onto nitrocellulose membranes (44). Both Western and dot blot membranes were blocked with 5% nonfat dry milk in TBS, pH 7.4, and incubated in primary antibodies overnight at 4 °C. For dot blots, 0.05% Triton X-100 was added to the TBS solution. The Tau12 (45), Tau5 (46), Tau7 (47), MOAB-2,[3] and TOC1 mouse monoclonal antibodies were used at 0.0067, 0.01, 0.04, 0.05, and 0.1 μg/ml, respectively. The mouse monoclonal anti-α-synuclein (Chemicon; MAB5320) and rabbit monoclonal anti-β-actin (Cell Signaling Technology; clone 13E5) antibodies were diluted to 1:2000 and 1:1000, respectively. The rabbit polyclonal antibodies R1 (48) and His-probe (Santa Cruz Biotechnology; clone H-15) were used at 0.0075 and 0.5 μg/ml, respectively. After rinsing, the membranes were incubated in peroxidase-conjugated horse anti-mouse secondary antibody (Vector Labs) or peroxidase-conjugated goat anti-rabbit (Vector Labs) secondary antibody for 1 h at room temperature. Reactivity was visualized using ECL substrate (Pierce). Dot blots were quantified using ImageJ software (National Institutes of Health) and expressed as the ratio of TOC1:Tau12 or TOC1:His probe intensity.

Immunogold Labeling of Recombinant Tau Aggregates

Aggregated Tau samples were spotted onto 300-mesh formvar/carbon-coated nickel grids (Electron Microscopy Sciences), blocked with 0.1% gelatin, 5% goat serum in TBS, and incubated with the His probe (Santa Cruz; 10 μg/ml) or TOC1 (50 μg/ml) primary antibodies in 5% goat serum/TBS. Grids were then rinsed with TBS prior to incubation with 10-nm diameter gold-conjugated anti-rabbit IgG (Sigma) or anti-mouse IgM (Electron Microscopy Sciences) secondary antibodies diluted 1:20 in 5% goat serum/TBS. Finally, grids were rinsed with ×10 TBS to reduce nonspecific labeling, rinsed with H_2O, and stained with 2% uranyl acetate. Samples were not fixed with glutaraldehyde because this obscured the TOC1 epitope.[4] Optimas 6.0 imaging software (Media Cybernetics) was used to identify and measure oligomers (defined as objects <50 nm in length) and filaments (defined as structures >50 nm in length) and individual gold particles were tallied. To control for differences in the relative quantities of oligomers and filaments present in a given Tau aggregation reaction, results were expressed as the ratio of TOC1:His tag labeling of the respective oligomeric or filamentous structures. Three fields from each grid were chosen for quantitation.

Immunohistochemistry

Tissue sections (40 μm) of control (Braak stages I and II) and severe AD (Braak stages V and VI) cases from the entorhinal cortex ($n = 4$), hippocampus ($n = 3$; AD only), and superior temporal gyrus ($n = 2$) were obtained from the Cognitive Neurology and Alzheimer's Disease Center at Northwestern University. Tissue sections were processed as previously described (49). The TOC1 antibody (0.05 μg/ml) was incubated with tissue sections overnight at 4 °C. The tissue was incubated in biotinylated goat anti-mouse secondary antibody (Vector; diluted 1:500) for 2 h followed by incubation in ABC solution (Vector; according to the manufacturer's instructions) for 1 h. The staining was developed with 3,3′-diaminobenzidine (Sigma). Sections were mounted onto glass slides, dehydrated through graded alcohols, cleared in xylenes, and coverslipped with Permaslip (Alban Scientific).

Immunofluorescence

Tissue sections (as described above) from the entorhinal cortex of control (Braak stages I and II; $n = 2$) and severe AD (Braak stages V and VI; $n = 2$) cases were processed for immunofluorescence using methods similar to those previously described (50). Briefly, sections were incubated with TOC1 (0.2 μg/ml), the rabbit monoclonal antibody pS^{422} (Epitomics; diluted 1:2500), and/or MN423 (0.5 μg/ml) (51) overnight at 4 °C. After washing with PBS containing 0.04% Triton X-100, sections were incubated in Alexa Fluor 488 goat anti-mouse IgM μ chain-specific (Invitrogen, diluted 1:500), Alexa Fluor 594 goat

[3] MOAB-2 is a mouse monoclonal antibody produced in the Binder laboratory that recognizes Aβ40 and -42; it is an IgG1.

[4] K. R. Patterson and L. I. Binder, unpublished observation.

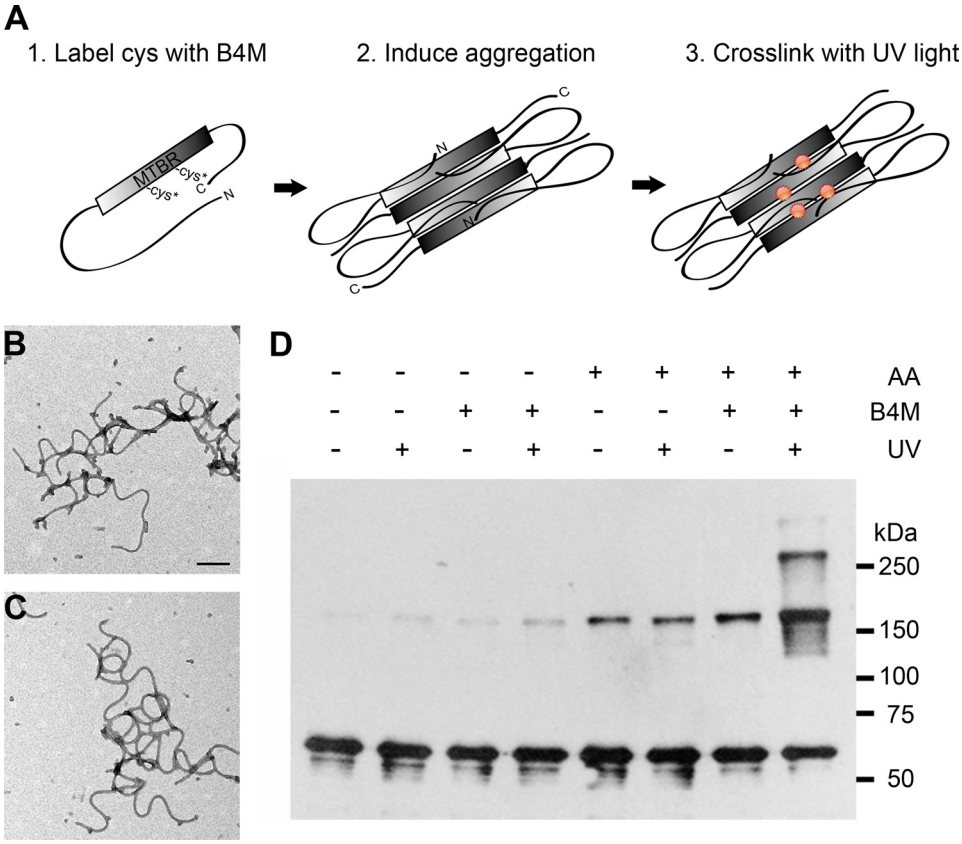

FIGURE 1. **Cross-linking Tau aggregates with B4M cross-linkers.** *A*, photochemical cross-linking was performed by incubating soluble Tau with B4M. Full-length Tau (hTau40) possesses two native cysteine (Cys) residues located in the 2nd and 3rd MTBRs. After conjugating the maleimide moiety of B4M to the native cysteines (*Cys**), aggregation of Tau was induced using AA and the resultant Tau aggregates were cross-linked with short-wave UV light. Aggregation-competent Tau is depicted in the Alz-50 conformation in which the N terminus comes into close proximity of the MTBR region (35). *Red circles* indicate potential cross-linked sites. *B*, EM of aggregated Tau with no cross-linker and no UV treatment. *Scale bar* is 200 nm. *C*, EM of B4M-conjugated Tau UV irradiated for 5 min is morphologically identical to untreated Tau. *D*, Western blot of cross-linked Tau filaments and controls. Cross-linking of Tau aggregates reveals an apparent 180-kDa multimer, as well as larger cross-linked products. Note the background levels of the 180-kDa multimer in the absence of cross-linking. 500 ng of Tau was loaded per lane and blotted with R1. Results are representative of five independent experiments.

anti-rabbit IgG (Invitrogen, diluted 1:500), and/or Alexa Fluor 594 goat anti-mouse IgG2b (Invitrogen, diluted 1:500) secondary antibodies for 2 h at room temperature. Sections were counterstained with Thiazin Red (0.004%) as indicated. Tissue sections were rinsed in PBS/Triton X-100, mounted onto glass slides, incubated with Sudan Black (0.05%) to eliminate lipofuscin autofluorescence, and coverslipped using Vectashield mounting medium (Vector). Staining was visualized using a LSM 510 Meta (Zeiss) laser scanning confocal microscope. All confocal images were acquired as z-stacks of single optical sections and analyzed using Zeiss LSM Image Viewer.

Statistics

SigmaStat software (Systat Software, Inc.) was used for all statistical tests. Comparisons were made using a *t* test or one-way analysis of variance followed by Student-Newman-Keuls post hoc analysis as indicated. Data were expressed as mean ± S.E. and significance was set at *p* values as noted.

RESULTS

Cross-linking of the Longest Isoform of Tau (hTau40) Reveals an Apparent 180-kDa Oligomer—We employed an established photochemical cross-linking method to examine intermolecular interactions of full-length Tau *in vitro* (52) (Fig. 1*A*). The B4M cross-linker is distinctive in that one end reacts with native cysteine residues and the other end is UV-photoactivatable. Thus, B4M can be used to label the cysteine residues prior to aggregation and then UV light can induce cross-linking of carbon-hydrogen bonds within 9 Å after the assembly reaction is complete (52). This substantially differs from previous work in which the cysteine residues are cross-linked and then Tau is polymerized into filamentous aggregates (26). In addition, using B4M eliminates accessibility issues that may arise when Tau is aggregated prior to cross-linking. B4M cross-linking did not affect the ability of Tau to aggregate (Fig. 1, *B* and *C*), allowing for the stabilization of Tau in its aggregation-competent conformation.

Treatment with an anionic inducing agent such as AA reveals sharp bands at apparent molecular masses of 180 kDa and higher when analyzed by SDS-PAGE (Fig. 1*D*). As monomeric hTau40 (actual molecular mass 47 kDa) migrates at 60 kDa on SDS-PAGE, this cross-linked product exhibits the apparent mass of a trimer. Importantly, only a small amount of this species is present in the absence of inducer. Moreover, background levels of the 180-kDa species are observed in the absence of

cross-linker indicating that this oligomeric species is somewhat SDS stable. To ensure that our results were not an artifact of our reaction conditions, we varied the UV irradiation time, Tau concentration, and AA concentration (supplemental Fig. S1). Under all conditions tested, the 180-kDa multimer was the predominant cross-linked species.

The 180-kDa Oligomeric Species Is Found in AD but Not Controls—Frontal cortex homogenates from severe AD (Braak V and VI; $n = 4$) and control cases with no cognitive impairment (Braak I–III; $n = 4$) were analyzed for the presence of SDS-stable Tau oligomeric aggregates. Interestingly, we found the 180-kDa species in all four AD cases examined but not the control cases (Fig. 2). Given that cleavage of Tau occurs in AD (53–55), we probed the homogenates for intact Tau using antibodies to the extreme N and C termini (Tau12 and Tau7, respectively) and found that the 180-kDa aggregates possess both termini and likely are not composed of cleavage products. When cross-linked recombinant Tau aggregates were run in parallel, the 180-kDa aggregates from brain and recombinant Tau samples appeared to migrate similarly (Fig. 2). These data demonstrate that SDS-stable Tau oligomers are disease specific and that the *in vitro* cross-linking method stabilizes Tau aggregates of comparable size.

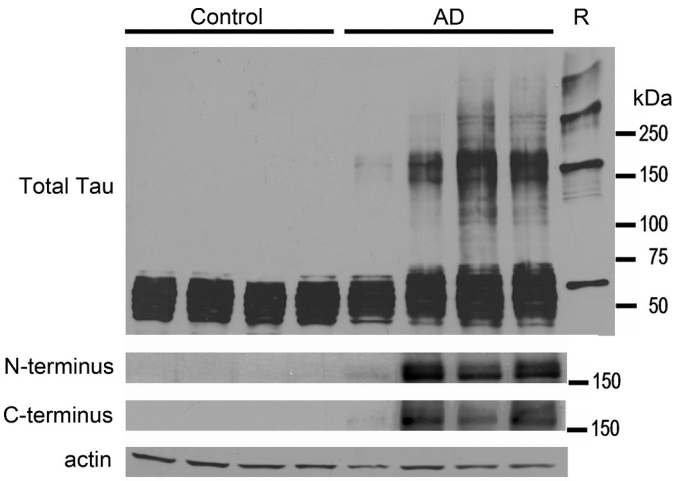

FIGURE 2. **An apparent 180-kDa Tau oligomer is found in Alzheimer disease but not in controls.** Whole homogenates (35 μg/lane) of frontal cortices obtained from 4 control and 4 AD brains were analyzed for the multimeric Tau species by Western blotting using polyclonal Tau antibody R1 (*total Tau*). Recombinant B4M cross-linked hTau40 (*R*) was run in parallel. In AD cases, multimeric Tau aggregates migrate at a similar M_r to cross-linked recombinant Tau indicating that these aggregated species may be comparable in nature. Multimeric Tau aggregates were not observed in control cases. Additionally, the 180-kDa multimeric Tau aggregate was visible in AD cases when probed with Tau12 (N terminus) and Tau7 (C terminus), indicating that this species is not an amalgam of cleavage products of Tau monomers. Actin was used as a loading control.

The 180-kDa Cross-linked Species Is a Dimer—Cross-linked recombinant Tau aggregates were sedimented to remove residual unaggregated Tau, dissociated with 2% SDS, and separated by SDS-PAGE. Monomeric Tau (~60 kDa on SDS-PAGE) and the 180-kDa cross-linked product were purified via electroelution. During purification of the 180-kDa cross-linked species, it was subjected to harsh denaturing conditions using SDS to dissociate noncovalent interactions. After purification, the 180-kDa product was analyzed via SDS-PAGE to verify that it still migrated at the same molecular mass (Fig. 3*A*). Variable amounts of monomeric Tau were co-eluted with the 180-kDa band, signifying that not all of the apparent 180-kDa products are cross-linked. Attempts to purify significant quantities of larger cross-linked species were unsuccessful.

SELDI-TOF MS of the electroeluted monomer revealed a prominent peak at 47 kDa as predicted (Fig. 3*B*). Smaller peaks at 94 and 141 kDa corresponding to dimeric and trimeric Tau species were also observed. In contrast, SELDI-TOF analysis of the purified apparent 180-kDa species revealed a prominent Tau dimer peak at 94 kDa in addition to the 47-kDa peak representing uncross-linked monomer (Fig. 3*C*). Minor trimer (141 kDa) and tetramer (188 kDa) peaks were also observed (supplemental Fig. S2). It is improbable that the dimeric Tau identified here is a breakdown product of the purified apparent 180-kDa cross-linked product because, if that were the case, we would expect to see another band that migrates at a molecular mass between the monomeric and 180-kDa species on SDS-PAGE. Thus, the cross-linked product is a dimer that migrates

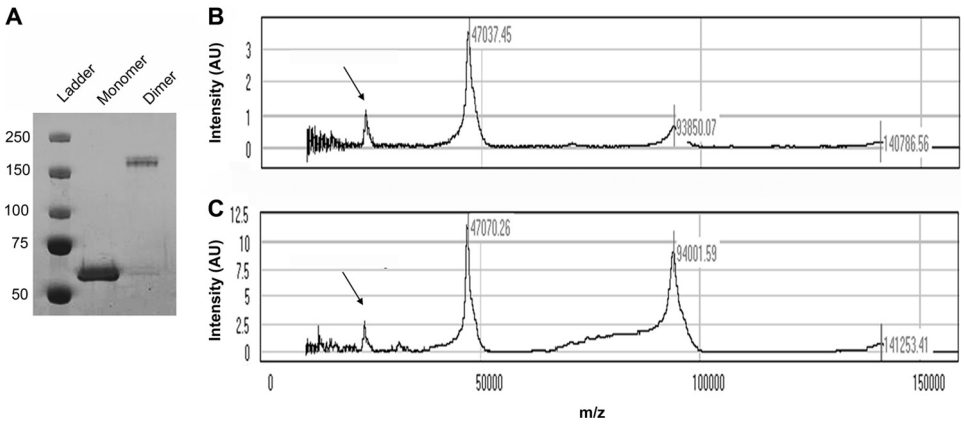

FIGURE 3. **SELDI-TOF MS analysis reveals that the apparent 180-kDa cross-linked product is predominantly a dimer.** *A*, cross-linked hTau40 aggregates were concentrated and separated by SDS-PAGE. Monomer and oligomer bands were extracted and electroeluted and then run on SDS-PAGE followed by staining with Coomassie Brilliant Blue R-250 to verify separation. *B*, SELDI-TOF MS analysis of Tau monomer reveals a peak at 47 kDa, the mass of hTau40. Additionally, minor peaks at 94 and 141 kDa were observed. *C*, SELDI-TOF MS analysis of the apparent 180-kDa cross-linked product reveals the prominent peak as 94 kDa, which corresponds to a dimer. Noticeably, a large Tau monomer peak is also present, likely representative of uncross-linked SDS-stable dimers that have since become dissociated. Monomer +2 charge peaks are denoted by *arrows*.

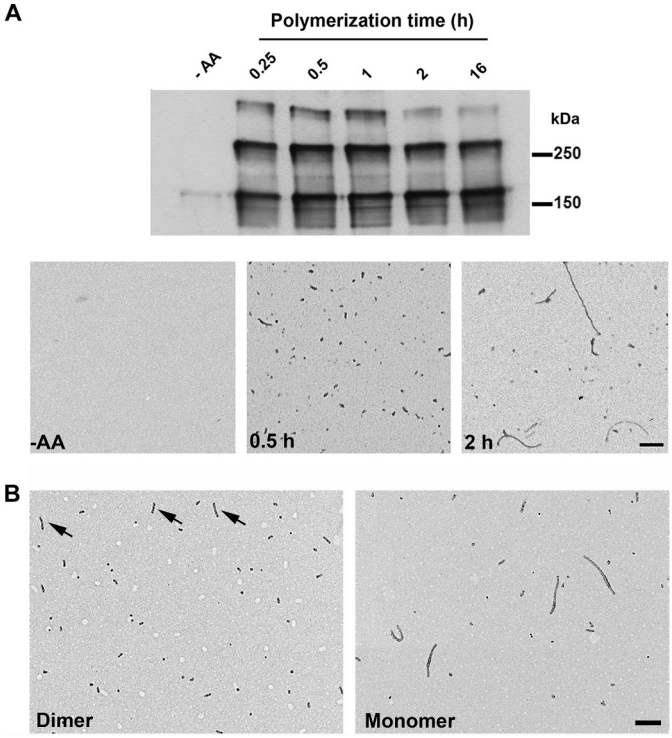

FIGURE 4. **Tau dimers associate to form oligomers but not long filaments.** *A*, Tau was cross-linked at defined time points after the addition of AA. Note that dimer cross-linking saturates 0.25 h after the onset of aggregation. Corresponding EMs demonstrate that long filaments do not emerge until after dimer formation has already saturated. *B*, EMs of purified dimer (4 μM total Tau equivalent to 2 μM dimeric Tau) and monomer (2 μM) 24 h after the addition of AA demonstrates that dimer aggregation produces mostly oligomers and a few short filaments (*arrows*). Conversely, electroeluted monomer forms long filaments in addition to oligomers when induced to aggregate with AA. Protein loading was 500 ng/lane blotted with R1. *Scale bars* in *A* and *B* are 200 nm.

anomalously when analyzed by SDS-PAGE most likely due to the anisotropy of these stable multimers.

Tau Dimers Aggregate to Form Oligomers but Not Long Filaments—Cross-linked Tau aggregates were sedimented to confirm that these species incorporate into larger aggregates. In the absence of inducer, the small amount of dimer present was found only in the supernatant (supplemental Fig. S3). In the presence of AA, all of the cross-linked species sediment indicating that they incorporate into larger Tau aggregates. This reveals that dimers are intermediates in at least some form of Tau aggregation as they are observed in the supernatant without inducer and the pellet after AA is added.

Time course experiments were performed to determine when dimer formation occurs. Tau dimerization reached peak levels 15 min after the addition of AA (Fig. 4*A*). Interestingly, only oligomers and the occasional short filament but no long filaments were observed at the earliest time points. Filament length steadily increased over the next several hours; however, a concomitant increase in dimerization was not observed. This indicates that dimerization is an early event that precedes filament formation *in vitro*.

To further ascertain the role of dimer formation, we aggregated purified cross-linked Tau dimers in the presence of AA (Fig. 4*B*). Similar to the early time points, mostly oligomeric aggregates were visible in the EM even 24 h after the addition of inducer. In contrast, assembly of electroeluted monomeric Tau resulted in the formation of oligomers *and* long filaments. Little aggregation of either monomeric or dimeric Tau was observed in the absence of AA.[5] Thus, it appears that Tau dimerization is a prenucleation event as AA is required for aggregation. It is possible that the oligomers composed of Tau dimers are "off-pathway" aggregates that do not incorporate into filaments; however, in the aggregated dimer preparations, a few short filaments were observed in addition to the oligomeric aggregates (Fig. 4*B*), suggesting that aggregated dimers can form filaments but that filament elongation likely favors a different mechanism of addition to the ends of the Tau polymer.

Tau Oligomeric Complex-1 (TOC1) Monoclonal Antibody Recognizes Tau Oligomers—Previous work demonstrated the existence of Tau oligomers in AD brain homogenates (25, 56); however, the role of these oligomers in disease remains controversial. To confirm that Tau dimers and/or higher order oligomeric species exist in AD, we raised a novel mouse monoclonal antibody, TOC1, against purified recombinant cross-linked Tau dimers. The selectivity of TOC1 for aggregated Tau over unaggregated Tau was confirmed using dot blots (Fig. 5, *A* and *B*). Importantly, when operating at saturating levels of antibody-immunogen binding, TOC1 showed no reactivity toward unaggregated Tau. In contrast, Tau12 reacted with both unaggregated and aggregated Tau. Furthermore, TOC1 failed to react with either α-synuclein or Aβ in the unaggregated, oligomeric, or filamentous states (Fig. 5*A*).

Next, we assessed the reactivity of TOC1 against purified cross-linked dimers. When probed using dot blots, TOC1 preferentially labeled cross-linked dimers over electroeluted B4M-labeled monomeric Tau isolated from the same aggregation reaction (Fig. 5*D*). These data indicated that the exposure to AA alone did not confer the TOC1 epitope and that a minimum of two Tau molecules was required to form the epitope.

To further clarify which aggregated species of Tau was recognized by TOC1, we used immunogold labeling of Tau aggregate preparations. Qualitative analyses of the electron micrographs revealed that TOC1 preferentially detected Tau oligomers over filaments; however, occasional labeling of the ends of filaments was observed (Fig. 6*A*). To control for concentration differences between oligomeric and filamentous aggregates, TOC1 immunogold labeling results were compared with immunogold labeling of the poly-His tag in the same aggregate preparation (Fig. 6*C*). TOC1 was over seven times more likely to label oligomers (structures $<$50 nm in length) than filaments (structures $>$50 nm in length). Collectively, these data establish that TOC1 is selective for Tau dimers and higher order oligomers but does not effectively label Tau monomers or filaments. Interestingly, TOC1 appears to label only a subpopulation of the oligomeric aggregates suggesting that more than one Tau oligomer conformation may exist.

TOC1 Recognizes a Conformational Epitope of Tau—The affinity data verifies that non-phosphorylated recombinant Tau possesses the necessary amino acid sequences for TOC1 binding but, unlike Tau12, the primary structure is not the only determinant of the interaction between oligomeric Tau and TOC1. To determine the amino acid sequences of Tau

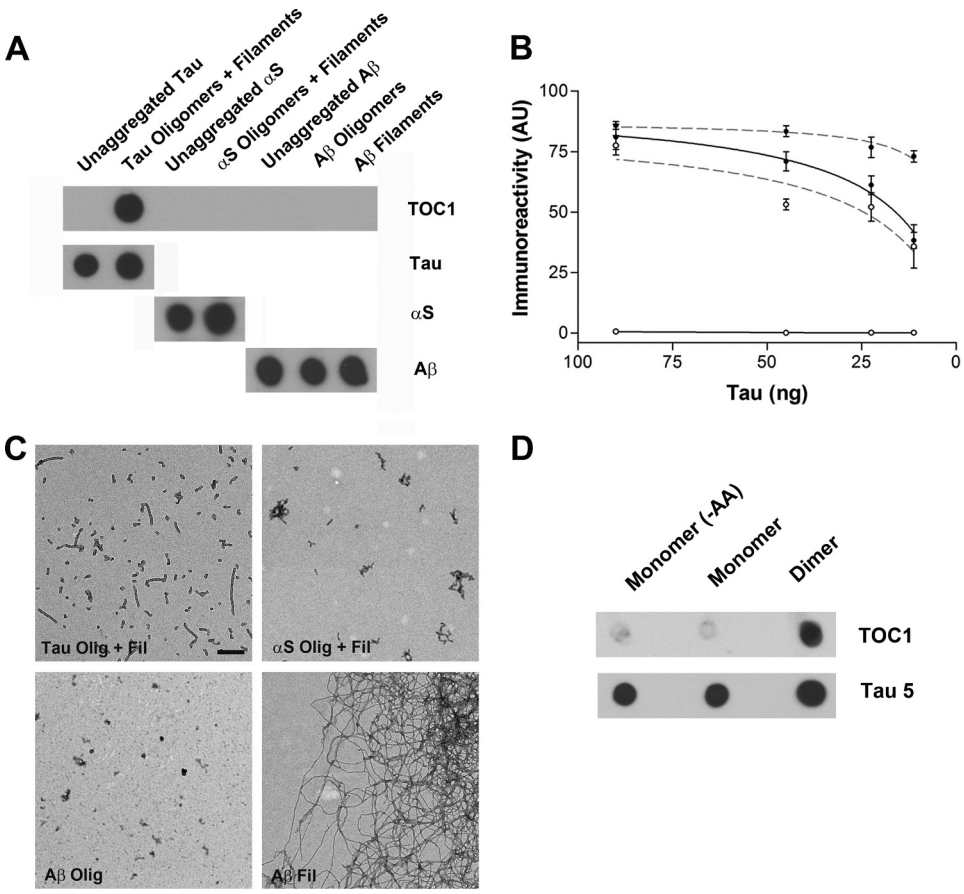

FIGURE 5. **Characterization of the TOC1 monoclonal Ab.** *A*, dot blot demonstrating TOC1 immunoreactivity. TOC1 preferentially labels uncross-linked Tau oligomeric and filamentous aggregates prepared with AA as opposed to unaggregated Tau (−*AA*). Moreover, TOC1 does not react with either α-synuclein (α*S*) or Aβ in the monomeric, oligomeric, or filamentous states. 45 ng/spot was applied to the nitrocellulose. Total Tau was determined using Tau12. *B*, quantification of TOC1 and Tau12 immunoreactivity at varying Tau concentrations. Whereas, Tau12 (*gray dashed line*) demonstrates a high affinity for both unaggregated (○) and aggregated (●) Tau, TOC1 (*black solid line*) reacts exclusively with Tau aggregates. Each point represents a minimum of three independent measurements. *C*, EMs of Tau oligomers and filaments (Tau Olig + Fil), α-synuclein oligomers and filaments (αS Olig + Fil), Aβ oligomers (Aβ Olig), and Aβ filaments (Aβ Fil) confirm the generation of aggregates of the appropriate morphology for each protein. *Scale bar* is 200 nm. *D*, TOC1 preferentially reacts with Tau dimers on dot blots. Monomeric and dimeric Tau were isolated from the same aggregation reaction. Also included is an electroeluted monomeric sample that was never exposed to AA (−*AA*). 12 ng/spot was applied to the nitrocellulose.

that serve as epitopes of TOC1, a recombinant library containing internal deletions of hTau40 was utilized (Fig. 7*A*). As this antibody requires aggregation of Tau for reactivity, deletion mutants were aggregated with AA prior to screening (Fig. 7*B*). Our results suggest that TOC1 binding is mediated by two segments on Tau. The first region lies within the proline-rich region (Gly^{155}–Gln^{244}) and is absolutely necessary for TOC1 binding (Fig. 7*C*). Deletion of a second region (Leu^{376}–Ser^{421}) contained within the C-terminal portion of the protein causes ~50% reduction in TOC1 binding. Given that these two regions are on either side of the MTBR, the results are consistent with the formation of an antiparallel dimer (Fig. 7*D*).

The deletion of residues Cys^{291}–Arg^{349} also results in ~50% reduction of TOC1 signal. Because this deletion lacks a large portion of the MTBR domain, it is not surprising that it aggregates poorly in comparison with the other internal deletion mutants (Fig. 7*B*). Therefore, the presence of this region is necessary for Tau aggregation and deletion of this region likely obstructs the formation of the TOC1 epitope. As an additional control, we also tested a construct that possessed *only* the MTBRs (Gln^{244}–Glu^{372}), and TOC1 showed *no* affinity for this construct. This indicates that this antibody does not recognize the portion of the Tau aggregates possessing β-pleated sheets (57) in the absence of the rest of the Tau molecule. Nonetheless, we cannot entirely rule out the possibility that the MTBRs comprise part of the epitope.

A potential caveat of these experiments is that deletion of these amino acid sequences could alter the conformation of Tau in such a way as to obscure or prevent the formation of the TOC1 epitope potentially obfuscating our results. Therefore, future experiments will be necessary to refine this preliminary mapping of the TOC1 epitope.

TOC1 Immunoreactivity Is Elevated in AD—Using the TOC1 antibody, we examined control and AD brains for the presence of Tau oligomeric aggregates. Interestingly, Western blot analyses of AD homogenates or *in vitro* cross-linked Tau using TOC1 were unsuccessful.[5] This indicates that even if Tau dimers do not dissociate when treated with SDS, the TOC1 conformation is not preserved. Thus, frontal cortex homogenates of control and severe AD cases were probed using dot blots under *non-denaturing* conditions. TOC1 demonstrated a marked increase in selectivity for AD samples over controls (Fig. 8, *A* and *B*). These results not only demonstrate

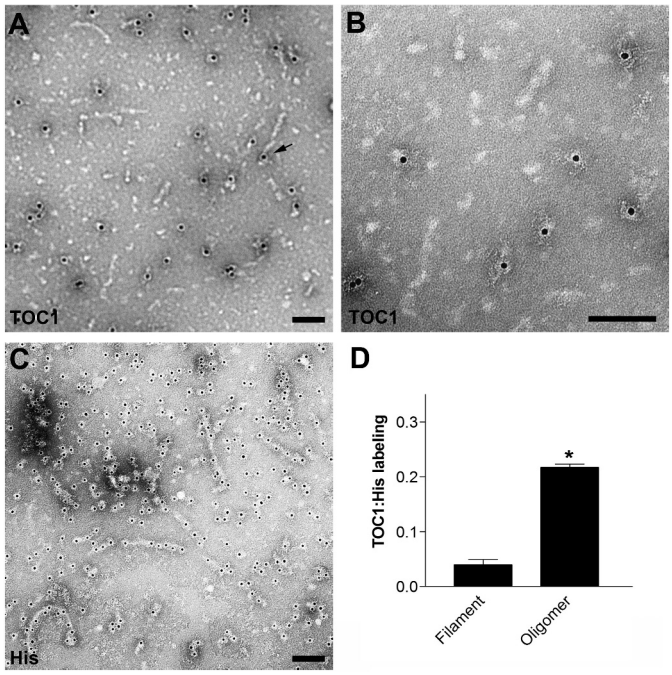

FIGURE 6. **TOC1 preferentially labels Tau oligomers.** *A*, TOC1 immunogold labeling reveals preferential labeling of oligomeric structures. However, labeling of the ends of a few filaments was observed as well (*arrow*). *B*, higher magnification of TOC1 immunogold labeling. *C*, immunogold labeling of the poly-His tag reveals abundant labeling of both Tau oligomers and filaments. *D*, quantification of TOC1 immunogold labeling of filaments (>50 nm) and oligomers (<50 nm) relative to His tag immunogold labeling of structures of the same category. *, $p < 0.01$, paired *t* test. *Scale bars* are 100 nm.

that Tau oligomers are elevated in AD but also validate the relevance of the TOC1 conformation to human disease.

To establish the spatial and temporal pattern of Tau oligomer formation in AD, TOC1 immunohistochemistry was performed on tissue sections from severe AD (Braak V and VI) and age-matched control cases (Braak I and II). Qualitative examination of sections from the entorhinal cortex, hippocampus, and superior temporal gyrus indicate that TOC1 reactivity follows the characteristic pattern of Braak staging (1) (Fig. 8). In control cases, TOC1 revealed neuropil threads as well as diffusely labeled neurons displaying both apical and basal dendritic processes (Fig. 8, *C–E*). These pretangle neurons are one of the earliest identifiable indicators of Tau deposition. As anticipated, a substantial increase in TOC1-positive inclusions was observed with increasing disease severity. In severe AD cases, TOC1 labels much of the classical Tau AD pathology, including neuropil threads, neuritic plaques, and neuronal pretangle and NFT-bearing inclusions (Fig. 8, *F–K*). These data indicate that Tau oligomerizaton is an early event in AD pathogenesis and that oligomers persist throughout the duration of the disease.

TOC1 Immunoreactivity Precedes NFT Formation—To further delineate the temporal pattern of Tau oligomer formation, we investigated whether TOC1 positive inclusions correlate with early or late stage markers of tangle evolution in AD. The phosphorylation of serine 422 (pS^{422}) on the Tau protein is an early modification in AD pathogenesis (58, 59). Thus, tissue sections from the entorhinal cortex of controls and severe AD cases were double-stained with TOC1 and pS^{422} antibodies using double label immunofluorescence. Qualitative observations revealed extensive colocalization of TOC1 and pS^{422} in both control and AD samples, and, as pathology progressed into AD, the amount of both TOC1 and pS^{422} reactivity increased (Fig. 9, *A* and *B*).

Next, we compared TOC1 immunofluorescence with that of a late stage NFT marker, MN423. MN423 recognizes Tau truncated at Glu^{391} (60). Qualitative analysis of severe AD cases revealed that TOC1 and MN423 reactivity are rarely observed in the same cell, indicating that the TOC1 epitope disappears prior to the truncation of Tau at residue 391 (Fig. 9*C*).

To establish whether or not TOC1 immunoreactivity is associated with mature NFTs, we performed immunofluorescence with TOC1 and Thiazin Red (TR). TR is a fluorescent dye that recognizes β-pleated sheet conformation in the neurofibrillary pathology of AD (61). We used the criteria of TR staining to differentiate between neurons containing seemingly more mature NFTs and those containing granular diffuse aggregates of Tau characteristic of early pretangle neurons. Interestingly, in areas possessing abundant TR-positive pathology, TOC1 predominantly labeled dystrophic neurites and neuropil threads but did not colocalize with TR (Fig. 9*D*). Occasionally, TOC1 labeled cells containing TR positive NFT pathology; however, TOC1 was primarily confined to the periphery of the tangles in these instances. Taken together, these data indicate that Tau oligomer formation represents an early event in AD pathogenesis that precedes neurofibrillary degeneration.

DISCUSSION

NFTs, a pathological hallmark of AD, are composed of Tau aggregates in the form of paired-helical filaments and straight filaments (62, 63). Although the spatiotemporal distribution of NFTs correlates with neuron loss and cognitive impairment in AD, current evidence suggests that NFTs may not be the primary form of Tau underlying neuronal dysfunction. For instance, the amount of neuronal loss greatly surpasses the amount of tangle formation in AD (64). Furthermore, neuronal loss and cognitive deficits precede neurofibrillary pathology in transgenic mouse models (20, 21). Consequently, it has been proposed that prefibrillar Tau aggregates may be responsible for a large part of disease-related neurotoxicity. To this effect, prefibrillar Tau aggregates correlate with cognitive dysfunction in a tauopathy mouse model, and similar multimeric Tau species were found in AD (25). In this study, we identify and characterize prefibrillar Tau aggregates that may be associated with disease-related cognitive decline in AD. We demonstrate that dimerization is an early event in the Tau aggregation process and that dimers are building blocks for prefibrillar oligomeric species. Furthermore, using a novel antibody, we provide the first glimpse of Tau oligomers within the context of early AD pathology.

One obstacle to studying Tau aggregation *in vitro* is that, unlike Aβ and α-synuclein, Tau does not aggregate spontaneously under physiological conditions (65). Anionic inducer molecules such as free fatty acids (*e.g.* AA) (66), heparin (67), or

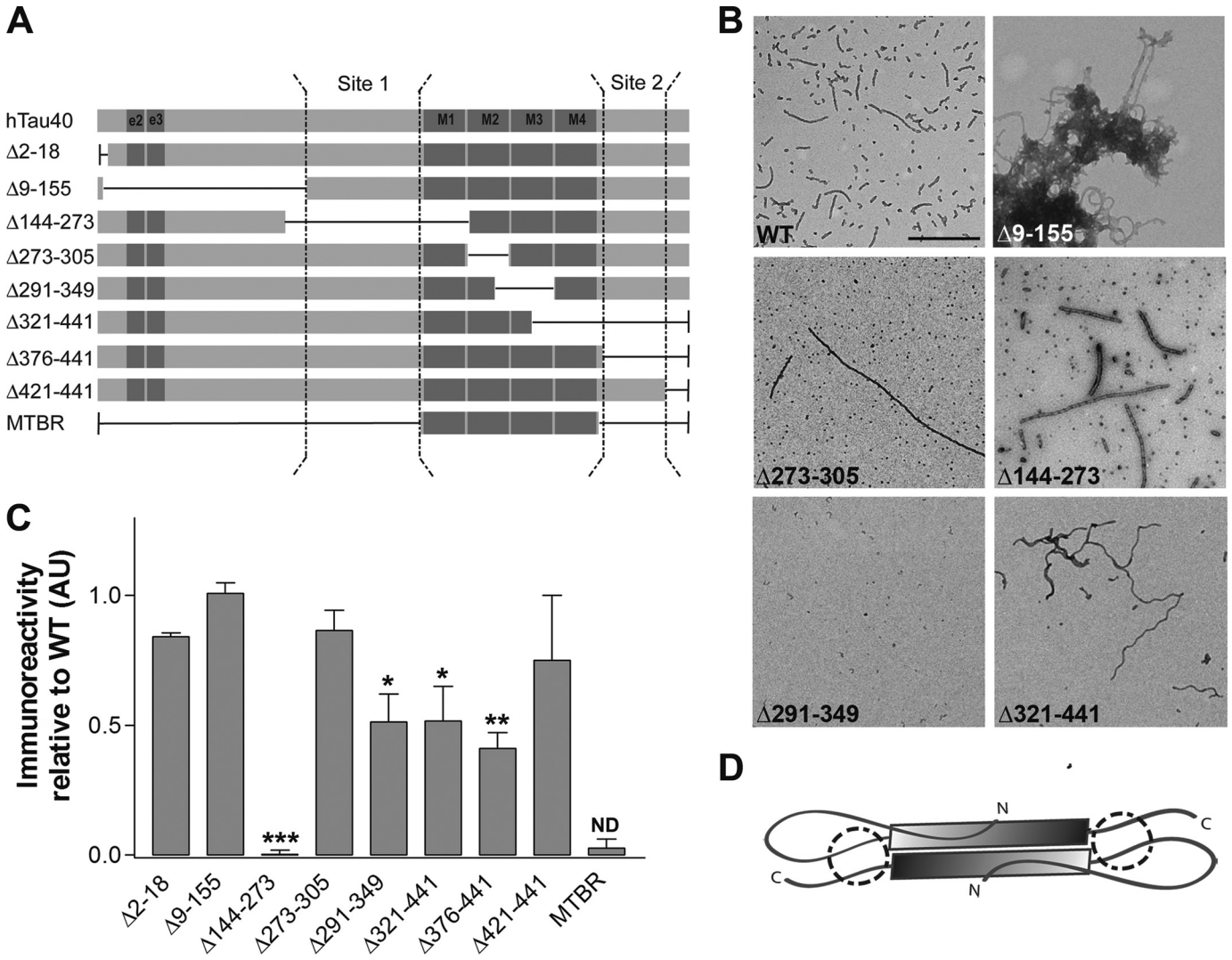

FIGURE 7. **Epitope mapping of TOC1.** Deletion mutants of hTau40 were assembled with AA, spotted onto nitrocellulose, and probed with TOC1. *A*, schematic representations of the deletion mutants utilized. *B*, EM of wild type (*WT*), Δ9–155, Δ273–305, Δ144–273, Δ291–349, and Δ321–441 hTau40 was used to confirm the presence of aggregates. The morphological characteristics of the other deletion mutants are described elsewhere (30, 36, 37, 53). *Scale bar* is 500 nm. *C*, immunoreactivity of TOC1 to deletion mutants of hTau40 expressed as the ratio of TOC1:total Tau. Total Tau was measured with either Tau12 or a His probe antibody. Results are normalized to WT hTau40. Each *bar* represents the average of three independent experiments with the exception of MTBR ($n = 2$). The proposed discontinuous epitope of TOC1 consists of residues 155–244 (Site 1) and residues 376–421 (Site 2) and is represented schematically in *panel A*. *, $p < 0.05$; **, $p < 0.01$; ***, $p < 0.001$, one-way analysis of variance; *ND*, *p* value not determined. *D*, the discontinuous epitope of TOC1 and its preferential binding to dimeric over monomeric Tau are consistent with an antiparallel dimer conformation. The *gray shaded box* represents the MTBR, and the proposed TOC1 epitope is *circled*.

RNA (68) are required to induce Tau polymerization *in vitro*; however, the physiological inducer of Tau aggregation *in situ* remains unknown. Using AA combined with a photochemical cross-linking technique, we stabilized Tau multimers that approximate those seen in AD when analyzed by SDS-PAGE. Tau multimers (*e.g.* dimers, trimers, etc.) are described elsewhere; however, previous work primarily focused on intermolecular associations mediated by disulfide bonds (29, 31, 69). Although three-repeat Tau possesses a single cysteine residue, four-repeat Tau has two cysteine residues favoring intramolecular over intermolecular disulfide bonds (30, 31). Furthermore, multiple reports affirm that reduction-resistant Tau multimers are present in AD and frontotemporal dementia (25, 70). Here, we utilized a benzophenone cross-linking technique that does not depend upon disulfide bridges. This technique has several advantages: (*a*) site-specific labeling of native cysteine residues, while Tau is in its soluble, extended conformation; (*b*) lack of interference with the Tau aggregation process; and (*c*) generation of stable, irreversible cross-linking of Tau multimers allowing for downstream applications such as aggregation and toxicity studies.

Although the existence of Tau multimeric aggregates in AD brain homogenates has been reported (25, 29, 56), the composition of these aggregates remains controversial. Previous studies suggest that Tau dimers are created when inducers such as heparin (29, 31) or thioflavin S (26) are used, and even in the absence of inducers (29, 71, 72), whereas others suggest Tau oligomers are composed of trimeric subunits (28). However, all of these previous conclusions were based on molecular weight estimations with SDS-PAGE, gel filtration chromatography, and/or mathematical modeling. Because Tau binds anomalously to SDS and exists as a non-globular protein, mass estima-

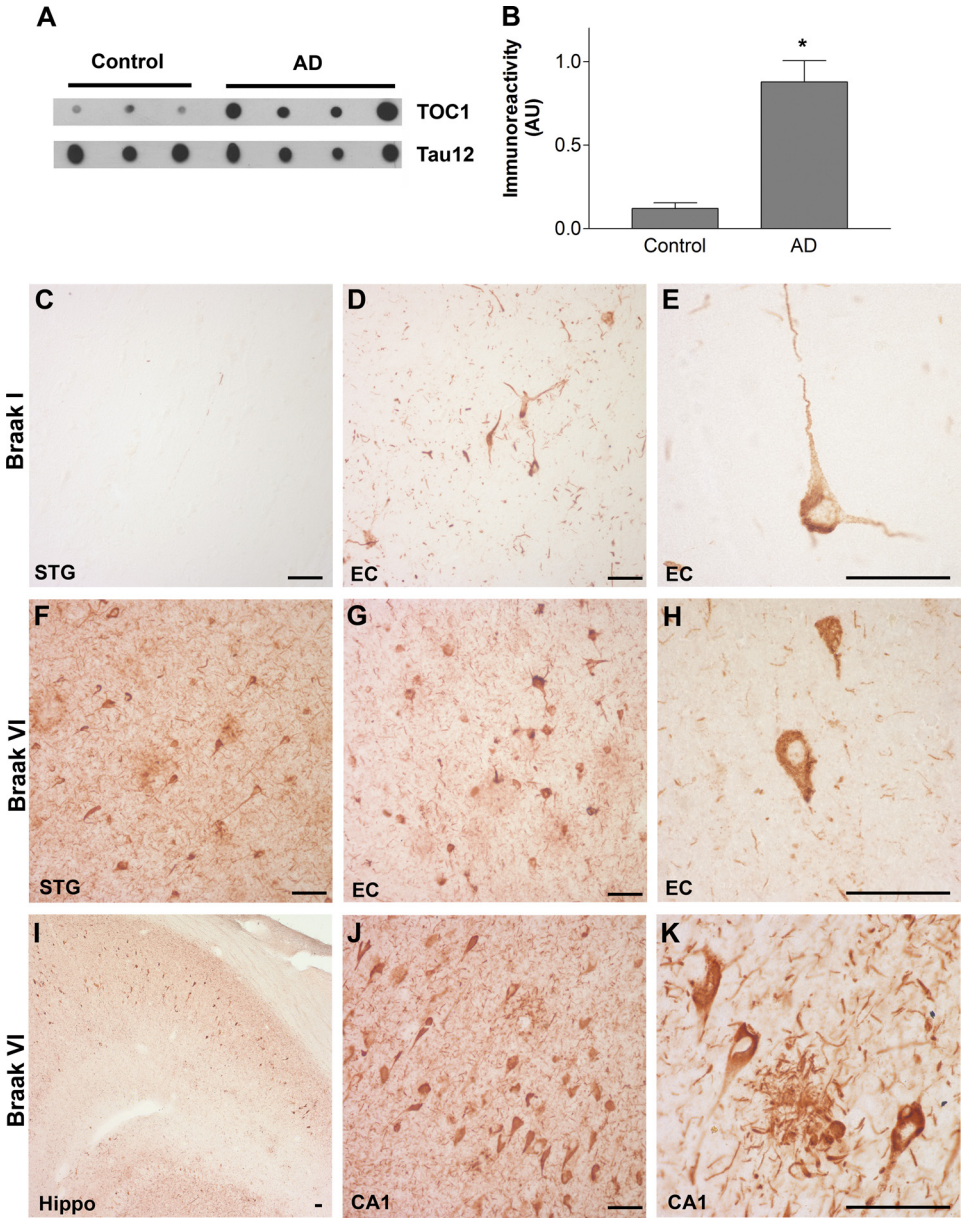

FIGURE 8. **TOC1 immunoreactivity is elevated in AD.** *A*, TOC1 preferentially labels Tau in AD brains compared with that from controls in non-denaturing conditions on dot blots (580 ng/spot) indicating that Tau in the TOC1 conformation is more abundant in AD. *B*, quantification of TOC1 labeling in extracts from the frontal cortex of control and AD brains in *A* represented as TOC1:Tau12 ratios. *, $p < 0.01$, unpaired *t* test. *C*, as expected, the superior temporal gyrus (*STG*) does not contain TOC1 immunoreactive Tau pathology in control cases (Braak I and II). *D*, in the entorhinal cortex (*EC*) of control cases, TOC1 labels early pretangle neurons with staining extending into both apical and basal dendritic processes. In addition, neuropil threads are labeled with TOC1. *E*, higher magnification of TOC1-labeled pretangle neuron in the EC from a control case reveals that these neurons do not contain mature compact NFTs. *F*, TOC1 labels abundant pathology in the STG of AD cases (Braak V and VI), including neuropil threads, neuritic plaques, as well as pretangle and tangle-bearing neurons. *G*, in the EC of AD cases, TOC1 labels similar pathology in addition to neurons that have lost their dendritic processes indicating that they are further along in the process of tangle evolution. *H*, higher magnification of TOC1 staining of the EC in AD. *I*, low magnification TOC1 immunostaining of the hippocampus of an AD case. *J*, TOC1 immunostaining in the CA1 region of the hippocampus in AD reveals flame-shaped inclusions within pyridimal neurons that are characteristic of this region. *K*, higher magnification of TOC1 immunolabeling of a neuritic plaque and pyramidal neurons in the CA1 region of an AD case. *Scale bars* are 50 μm.

tion using these techniques can be inaccurate (73). Therefore, we utilized SELDI-TOF mass spectrometry to analyze the cross-linked apparent 180-kDa multimer to provide a more definitive measurement of the molecular mass of this aggregate. Our data clearly demonstrate that this aggregate is in fact a dimer.

We demonstrate that dimeric aggregates occur in the absence of cross-linker and even, to some extent, in the absence of inducer; however, B4M cross-linking obviously stabilizes these aggregates. In AD, Tau is cross-linked by transglutaminases and products of lipid peroxidation such as hydroxynonenal (product of AA peroxidation), and these modifications may even promote Tau aggregation by stabilizing AD-associated Tau conformations such as Alz-50 (74–79). Although it is likely that Tau dimerization occurs under physiological conditions, the process may become dysregulated in disease. Formation of stable cross-links may be one mechanism by which the equilibrium shifts away from soluble, monomeric Tau toward Tau aggregates.

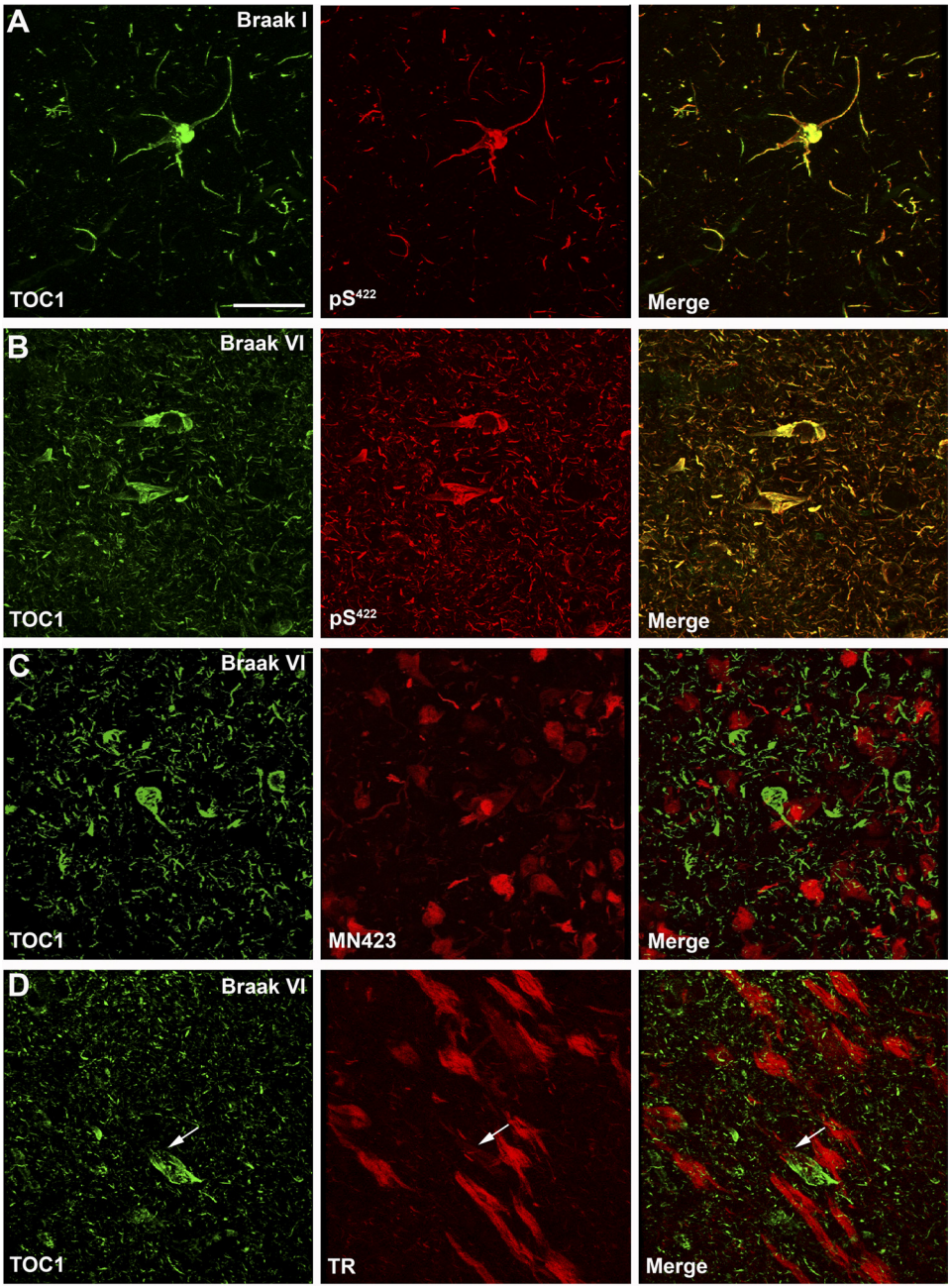

FIGURE 9. **TOC1 immunoreactivity colocalizes with early markers of Tau pathology.** *A* and *B*, laser scanning confocal microscopy was used to determine the degree of colocalization between TOC1 (*green*) and pS^{422} (*red*) in the entorhinal cortex. Colocalization between the two antibodies was almost complete in both control (*A*) and AD (*B*) cases, indicating that formation of the TOC1 epitope correlates with phosphorylation of Ser^{422}, an early event in AD pathogenesis. *C*, immunofluorescence was performed using TOC1 (*green*) and MN423 (*red*) in severe AD cases. Very little colocalization was observed. *D*, in severe AD cases, TOC1 and TR did not colocalize, indicating that the TOC1 epitope precedes β-sheet formation characteristic of NFTs. Although occasional inclusions with both TOC1 and TR exist (*arrow*), different portions of the cell are labeled by each. *Scale bar* is 50 μm.

We show that dimerization is an early event in the Tau aggregation process, which precedes the formation of filaments. In fact, aggregation of purified Tau dimers resulted in the formation of oligomers and a few short filaments in contrast to the aggregation of monomeric Tau, which formed longer filaments. Stable filaments can form by a nucleation-elongation reaction in which monomers first form a stable nucleus (nucleation) to which additional monomers can add (elongation) (80). The nucleation process is critical and rate-limiting, as lowering this energy barrier induces the production of more filaments. Because Tau dimers did not self-associate in the absence of inducer, our findings suggest that Tau dimer formation precedes nucleation and that some other conformational shift must occur prior to oligomer and filament formation. A potential caveat is that the cross-linked Tau dimers were denatured during the purification process, and, thus, it is possible that the proteins did not re-nature completely or correctly. Moreover, our results indicate that dimeric Tau is not favored for elongation, at least not in the cross-linked form. It is possible that dimers that are not cross-linked have the freedom to rearrange into a conformation such that elongation could occur. Further studies are required to elucidate the events necessary for Tau

nucleation, and to determine whether dimers lead directly to oligomers and subsequent filament formation or whether these oligomers represent off-pathway aggregates that do not form filaments.

To validate the relevance of these findings to AD, we generated a novel monoclonal antibody that selectively labels Tau dimers and higher order oligomers. Interestingly, TOC1 immunoreactivity was greatly elevated in AD brains over controls. TOC1 avidly labeled the hallmark Tau pathology in AD including neuropil threads, neuritic plaques, and neuronal inclusions. Moreover, the presence of TOC1 immunoreactive inclusions in control cases (Braak stages I and II) suggests that dimer/oligomer formation is an early event in disease pathogenesis. Supporting this assertion, immunofluorescence in human tissue sections indicated that oligomerization closely associates with Ser^{422} phosphorylation, an early pathological event in AD (58). Moreover, colocalization with TR, a marker for fibrillar forms of both Tau and Aβ, and colocalization with MN423, a late NFT marker (60), was scarcely observed. These findings confirm that TOC1 does indeed label prefibrillar pathology. The presence of TOC1 positive prefibrillar inclusions in AD supports our *in vitro* Tau aggregation and cross-linking results suggesting that Tau dimers/oligomers may be intermediates in the aggregation process that precede NFT formation *in situ*.

AD is characterized by the presence of both Aβ and Tau inclusions; however, Tau is necessary for toxicity of Aβ in both cultured cells and transgenic mice (3, 4). Therefore, elucidating the mechanism by which Tau converts from a soluble, microtubule-bound protein into stable, toxic aggregates appears key to understanding this disease. Nonetheless, the link between Aβ and Tau aggregation remains enigmatic. Several studies have established that Aβ oligomers increase phospholipase A_2 activity, which in turn elevates AA resulting in neuronal toxicity (81–83). Increased activity of cytoplasmic phospholipase A_2 has been confirmed in AD, generating increased levels of free fatty acids including AA (84). Interestingly, reduction of phospholipase A_2 ameliorates cognitive deficits in an amyloid precursor protein mouse model of AD (83). In the same model, reduction of endogenous Tau also prevented behavioral deficits (4). These findings suggest that AA and Tau may work synergistically. Here we provide evidence that AA-stimulated Tau aggregation is relevant to AD, suggesting that the liberation of free fatty acids including AA is a potential link between Aβ and Tau pathology.

The discontinuous epitopes of antibodies provide evidence for conformational changes in Tau during the disease process. For instance, epitope mapping of the Alz-50 antibody reveals that the N terminus comes into close proximity to the MTBR *early* in tangle evolution (35, 85). TOC1 is also a conformation-selective antibody that appears to recognize portions of the proline-rich region and C terminus of Tau. It is possible that this epitope may occur from intramolecular folding events; however, because TOC1 does not recognize monomeric Tau, it is more likely that this is an intermolecular event consistent with the formation of anti-parallel dimers given that the two epitopes are on either side of the MTBRs (see Fig. 7). This expands upon a previous study showing that three-repeat Tau can dimerize in an antiparallel manner (72). Our results suggest that both three- and four-repeat Tau form antiparallel dimers; however, TOC1 labeled only a portion of the Tau aggregates, suggesting that there may be other aggregation-competent conformations to discover. Future studies are warranted to fully chart the evolution of the conformational shifts of Tau and how they relate to TOC1 during disease pathogenesis. Even so, our results confer significant insights concerning the earliest stages of Tau aggregation and provide an important foundation for the future study of potentially neurotoxic Tau oligomers in disease pathogenesis.

Acknowledgments—We thank Dr. Sarah E. Rice, Dr. Kristin Deitrich, and Isabella Ugwu for technical assistance. We also thank Dr. Nichole LaPointe for the α-synuclein preparation.

REFERENCES

1. Braak, H., and Braak, E. (1991) *Acta Neuropathol.* **82,** 239–259
2. Arriagada, P. V., Growdon, J. H., Hedley-Whyte, E. T., and Hyman, B. T. (1992) *Neurology* **42,** 631–639
3. Rapoport, M., Dawson, H. N., Binder, L. I., Vitek, M. P., and Ferreira, A. (2002) *Proc. Natl. Acad. Sci. U.S.A.* **99,** 6364–6369
4. Roberson, E. D., Scearce-Levie, K., Palop, J. J., Yan, F., Cheng, I. H., Wu, T., Gerstein, H., Yu, G. Q., and Mucke, L. (2007) *Science* **316,** 750–754
5. Vossel, K. A., Zhang, K., Brodbeck, J., Daub, A. C., Sharma, P., Finkbeiner, S., Cui, B., and Mucke, L. (2010) *Science* **330,** 198
6. Feany, M. B., and Dickson, D. W. (1996) *Ann. Neurol.* **40,** 139–148
7. Poorkaj, P., Bird, T. D., Wijsman, E., Nemens, E., Garruto, R. M., Anderson, L., Andreadis, A., Wiederholt, W. C., Raskind, M., and Schellenberg, G. D. (1998) *Ann. Neurol.* **43,** 815–825
8. Poorkaj, P., Grossman, M., Steinbart, E., Payami, H., Sadovnick, A., Nochlin, D., Tabira, T., Trojanowski, J. Q., Borson, S., Galasko, D., Reich, S., Quinn, B., Schellenberg, G., and Bird, T. D. (2001) *Arch. Neurol.* **58,** 383–387
9. Spillantini, M. G., Murrell, J. R., Goedert, M., Farlow, M. R., Klug, A., and Ghetti, B. (1998) *Proc. Natl. Acad. Sci. U.S.A.* **95,** 7737–7741
10. Hutton, M., Lendon, C. L., Rizzu, P., Baker, M., Froelich, S., Houlden, H., Pickering-Brown, S., Chakraverty, S., Isaacs, A., Grover, A., Hackett, J., Adamson, J., Lincoln, S., Dickson, D., Davies, P., Petersen, R. C., Stevens, M., de Graaff, E., Wauters, E., van Baren, J., Hillebrand, M., Joosse, M., Kwon, J. M., Nowotny, P., Che, L. K., Norton, J., Morris, J. C., Reed, L. A., Trojanowski, J., Basun, H., Lannfelt, L., Neystat, M., Fahn, S., Dark, F., Tannenberg, T., Dodd, P. R., Hayward, N., Kwok, J. B., Schofield, P. R., Andreadis, A., Snowden, J., Craufurd, D., Neary, D., Owen, F., Oostra, B. A., Hardy, J., Goate, A., van Swieten, J., Mann, D., Lynch, T., and Heutink, P. (1998) *Nature* **393,** 702–705
11. Schweers, O., Schönbrunn-Hanebeck, E., Marx, A., and Mandelkow, E. (1994) *J. Biol. Chem.* **269,** 24290–24297
12. Iqbal, K., Liu, F., Gong, C. X., Alonso Adel, C., and Grundke-Iqbal, I. (2009) *Acta Neuropathol.* **118,** 53–69
13. von Bergen, M., Friedhoff, P., Biernat, J., Heberle, J., Mandelkow, E. M., and Mandelkow, E. (2000) *Proc. Natl. Acad. Sci. U.S.A.* **97,** 5129–5134
14. Lewis, J., McGowan, E., Rockwood, J., Melrose, H., Nacharaju, P., Van Slegtenhorst, M., Gwinn-Hardy, K., Paul Murphy, M., Baker, M., Yu, X., Duff, K., Hardy, J., Corral, A., Lin, W. L., Yen, S. H., Dickson, D. W., Davies, P., and Hutton, M. (2000) *Nat. Genet.* **25,** 402–405
15. Götz, J., Chen, F., Barmettler, R., and Nitsch, R. M. (2001) *J. Biol. Chem.* **276,** 529–534
16. Tanemura, K., Akagi, T., Murayama, M., Kikuchi, N., Murayama, O., Hashikawa, T., Yoshiike, Y., Park, J. M., Matsuda, K., Nakao, S., Sun, X., Sato, S., Yamaguchi, H., and Takashima, A. (2001) *Neurobiol. Dis.* **8,** 1036–1045
17. Tatebayashi, Y., Miyasaka, T., Chui, D. H., Akagi, T., Mishima, K., Iwasaki, K., Fujiwara, M., Tanemura, K., Murayama, M., Ishiguro, K., Planel, E., Sato, S., Hashikawa, T., and Takashima, A. (2002) *Proc. Natl. Acad. Sci.*

U.S.A. **99,** 13896–13901
18. Allen, B., Ingram, E., Takao, M., Smith, M. J., Jakes, R., Virdee, K., Yoshida, H., Holzer, M., Craxton, M., Emson, P. C., Atzori, C., Migheli, A., Crowther, R. A., Ghetti, B., Spillantini, M. G., and Goedert, M. (2002) *J. Neurosci.* **22,** 9340–9351
19. Andorfer, C., Acker, C. M., Kress, Y., Hof, P. R., Duff, K., and Davies, P. (2005) *J. Neurosci.* **25,** 5446–5454
20. Oddo, S., Caccamo, A., Shepherd, J. D., Murphy, M. P., Golde, T. E., Kayed, R., Metherate, R., Mattson, M. P., Akbari, Y., and LaFerla, F. M. (2003) *Neuron* **39,** 409–421
21. Spires, T. L., Orne, J. D., SantaCruz, K., Pitstick, R., Carlson, G. A., Ashe, K. H., and Hyman, B. T. (2006) *Am. J. Pathol.* **168,** 1598–1607
22. Santacruz, K., Lewis, J., Spires, T., Paulson, J., Kotilinek, L., Ingelsson, M., Guimaraes, A., DeTure, M., Ramsden, M., McGowan, E., Forster, C., Yue, M., Orne, J., Janus, C., Mariash, A., Kuskowski, M., Hyman, B., Hutton, M., and Ashe, K. H. (2005) *Science* **309,** 476–481
23. Sydow, A., Van der Jeugd, A., Zheng, F., Ahmed, T., Balschun, D., Petrova, O., Drexler, D., Zhou, L., Rune, G., Mandelkow, E., D'Hooge, R., Alzheimer, C., and Mandelkow, E. M. (2011) *J. Neurosci.* **31,** 2511–2525
24. Wittmann, C. W., Wszolek, M. F., Shulman, J. M., Salvaterra, P. M., Lewis, J., Hutton, M., and Feany, M. B. (2001) *Science* **293,** 711–714
25. Berger, Z., Roder, H., Hanna, A., Carlson, A., Rangachari, V., Yue, M., Wszolek, Z., Ashe, K., Knight, J., Dickson, D., Andorfer, C., Rosenberry, T. L., Lewis, J., Hutton, M., and Janus, C. (2007) *J. Neurosci.* **27,** 3650–3662
26. Friedhoff, P., von Bergen, M., Mandelkow, E. M., Davies, P., and Mandelkow, E. (1998) *Proc. Natl. Acad. Sci. U.S.A.* **95,** 15712–15717
27. Congdon, E. E., Kim, S., Bonchak, J., Songrug, T., Matzavinos, A., and Kuret, J. (2008) *J. Biol. Chem.* **283,** 13806–13816
28. Lasagna-Reeves, C. A., Castillo-Carranza, D. L., Guerrero-Muoz, M. J., Jackson, G. R., and Kayed, R. (2010) *Biochemistry* **49,** 10039–10041
29. Sahara, N., Maeda, S., Murayama, M., Suzuki, T., Dohmae, N., Yen, S. H., and Takashima, A. (2007) *Eur. J. Neurosci.* **25,** 3020–3029
30. Barghorn, S., and Mandelkow, E. (2002) *Biochemistry* **41,** 14885–14896
31. Schweers, O., Mandelkow, E. M., Biernat, J., and Mandelkow, E. (1995) *Proc. Natl. Acad. Sci. U.S.A.* **92,** 8463–8467
32. Gamblin, T. C., King, M. E., Kuret, J., Berry, R. W., and Binder, L. I. (2000) *Biochemistry* **39,** 14203–14210
33. Lee, V. M., Goedert, M., and Trojanowski, J. Q. (2001) *Annu. Rev. Neurosci.* **24,** 1121–1159
34. Goedert, M., Spillantini, M. G., Potier, M. C., Ulrich, J., and Crowther, R. A. (1989) *EMBO. J.* **8,** 393–399
35. Carmel, G., Mager, E. M., Binder, L. I., and Kuret, J. (1996) *J. Biol. Chem.* **271,** 32789–32795
36. Abraha, A., Ghoshal, N., Gamblin, T. C., Cryns, V., Berry, R. W., Kuret, J., and Binder, L. I. (2000) *J. Cell Sci.* **113,** 3737–3745
37. Gamblin, T. C., Berry, R. W., and Binder, L. I. (2003) *Biochemistry* **42,** 2252–2257
38. Carmel, G., Leichus, B., Cheng, X., Patterson, S. D., Mirza, U., Chait, B. T., Kuret, J. (1994) *J. Biol. Chem.* **269,** 7304–7309
39. Gamblin, T. C., King, M. E., Dawson, H., Vitek, M. P., Kuret, J., Berry, R. W., and Binder, L. I. (2000) *Biochemistry* **39,** 6136–6144
40. Necula, M., Chirita, C. N., and Kuret, J. (2003) *J. Biol. Chem.* **278,** 46674–46680
41. Stine, W. B., Jungbauer, L., Yu, C., and LaDu, M. J. (2011) *Methods Mol. Biol.* **670,** 13–32
42. Binder, L. I., Frankfurter, A., and Rebhun, L. I. (1985) *J. Cell Biol.* **101,** 1371–1378
43. Reyes, J. F., Reynolds, M. R., Horowitz, P. M., Fu, Y., Guillozet-Bongaarts, A. L., Berry, R., and Binder, L. I. (2008) *Neurobiol. Dis.* **31,** 198–208
44. LaPointe, N. E., Morfini, G., Pigino, G., Gaisina, I. N., Kozikowski, A. P., Binder, L. I., and Brady, S. T. (2009) *J. Neurosci. Res.* **87,** 440–451
45. Horowitz, P. M., Patterson, K. R., Guillozet-Bongaarts, A. L., Reynolds, M. R., Carroll, C. A., Weintraub, S. T., Bennett, D. A., Cryns, V. L., Berry, R. W., and Binder, L. I. (2004) *J. Neurosci.* **24,** 7895–7902
46. LoPresti, P., Szuchet, S., Papasozomenos, S. C., Zinkowski, R. P., and Binder, L. I. (1995) *Proc. Natl. Acad. Sci. U.S.A.* **92,** 10369–10373
47. Horowitz, P. M., LaPointe, N., Guillozet-Bongaarts, A. L., Berry, R. W., and Binder, L. I. (2006) *Biochemistry* **45,** 12859–12866
48. Berry, R. W., Sweet, A. P., Clark, F. A., Lagalwar, S., Lapin, B. R., Wang, T., Topgi, S., Guillozet-Bongaarts, A. L., Cochran, E. J., Bigio, E. H., and Binder, L. I. (2004) *J. Neurocytol.* **33,** 287–295
49. Kanaan, N. M., Kordower, J. H., and Collier, T. J. (2007) *J. Comp. Neurol.* **502,** 683–700
50. Garcia-Sierra, F., Ghoshal, N., Quinn, B., Berry, R. W., and Binder, L. I. (2003) *J. Alzheimers Dis.* **5,** 65–77
51. Novak, M., Wischik, C. M., Edwards, P., Pannell, R., and Milstein, C. (1989) *Prog. Clin. Biol. Res.* **317,** 755–761
52. Dormán, G., and Prestwich, G. D. (1994) *Biochemistry* **33,** 5661–5673
53. Gamblin, T. C., Chen, F., Zambrano, A., Abraha, A., Lagalwar, S., Guillozet, A. L., Lu, M., Fu, Y., Garcia-Sierra, F., LaPointe, N., Miller, R., Berry, R. W., Binder, L. I., and Cryns, V. L. (2003) *Proc. Natl. Acad. Sci. U.S.A.* **100,** 10032–10037
54. Novak, M., Kabat, J., and Wischik, C. M. (1993) *EMBO J.* **12,** 365–370
55. Guo, H., Albrecht, S., Bourdeau, M., Petzke, T., Bergeron, C., and LeBlanc, A. C. (2004) *Am. J. Pathol.* **165,** 523–531
56. Maeda, S., Sahara, N., Saito, Y., Murayama, S., Ikai, A., and Takashima, A. (2006) *Neurosci. Res.* **54,** 197–201
57. Barghorn, S., Davies, P., and Mandelkow, E. (2004) *Biochemistry* **43,** 1694–1703
58. Guillozet-Bongaarts, A. L., Cahill, M. E., Cryns, V. L., Reynolds, M. R., Berry, R. W., and Binder, L. I. (2006) *J. Neurochem.* **97,** 1005–1014
59. Mondragón-Rodríguez, S., Basurto-Islas, G., Santa-Maria, I., Mena, R., Binder, L. I., Avila, J., Smith, M. A., Perry, G., and García-Sierra, F. (2008) *Int. J. Exp. Pathol.* **89,** 81–90
60. Guillozet-Bongaarts, A. L., Garcia-Sierra, F., Reynolds, M. R., Horowitz, P. M., Fu, Y., Wang, T., Cahill, M. E., Bigio, E. H., Berry, R. W., and Binder, L. I. (2005) *Neurobiol. Aging* **26,** 1015–1022
61. Luna-Muñoz, J., Peralta-Ramirez, J., Chávez-Macías, L., Harrington, C. R., Wischik, C. M., and Mena, R. (2008) *Acta Neuropathol.* **116,** 507–515
62. Kidd, M. (1963) *Nature* **197,** 192–193
63. Kosik, K. S., Joachim, C. L., and Selkoe, D. J. (1986) *Proc. Natl. Acad. Sci. U.S.A.* **83,** 4044–4048
64. Gómez-Isla, T., Hollister, R., West, H., Mui, S., Growdon, J. H., Petersen, R. C., Parisi, J. E., and Hyman, B. T. (1997) *Ann. Neurol.* **41,** 17–24
65. Chirita, C. N., Congdon, E. E., Yin, H., and Kuret, J. (2005) *Biochemistry* **44,** 5862–5872
66. Wilson, D. M., and Binder, L. I. (1995) *J. Biol. Chem.* **270,** 24306–24314
67. Pérez, M., Valpuesta, J. M., Medina, M., Montejo de Garcini, E., and Avila, J. (1996) *J. Neurochem.* **67,** 1183–1190
68. Kampers, T., Friedhoff, P., Biernat, J., Mandelkow, E. M., and Mandelkow, E. (1996) *FEBS. Lett.* **399,** 344–349
69. Guttmann, R. P., Erickson, A. C., and Johnson, G. V. (1995) *J. Neurochem.* **64,** 1209–1215
70. Maeda, S., Sahara, N., Saito, Y., Murayama, M., Yoshiike, Y., Kim, H., Miyasaka, T., Murayama, S., Ikai, A., and Takashima, A. (2007) *Biochemistry* **46,** 3856–3861
71. Rosenberg, K. J., Ross, J. L., Feinstein, H. E., Feinstein, S. C., and Israelachvili, J. (2008) *Proc. Natl. Acad. Sci. U.S.A.* **105,** 7445–7450
72. Wille, H., Drewes, G., Biernat, J., Mandelkow, E. M., and Mandelkow, E. (1992) *J. Cell Biol.* **118,** 573–584
73. Cabré, F., Canela, E. I., and Canela, M. A. (1989) *J. Chromatogr.* **472,** 347–356
74. Sayre, L. M., Zelasko, D. A., Harris, P. L., Perry, G., Salomon, R. G., and Smith, M. A. (1997) *J. Neurochem.* **68,** 2092–2097
75. Liu, Q., Smith, M. A., Avilá, J., DeBernardis, J., Kansal, M., Takeda, A., Zhu, X., Nunomura, A., Honda, K., Moreira, P. I., Oliveira, C. R., Santos, M. S., Shimohama, S., Aliev, G., de la Torre, J., Ghanbari, H. A., Siedlak, S. L., Harris, P. L., Sayre, L. M., and Perry, G. (2005) *Free Radic. Biol. Med.* **38,** 746–754
76. Appelt, D. M., and Balin, B. J. (1997) *Brain Res.* **745,** 21–31
77. Balin, B. J., and Appelt, D. M. (2000) *Methods Mol. Med.* **32,** 395–404
78. Dudek, S. M., and Johnson, G. V. (1993) *J. Neurochem.* **61,** 1159–1162
79. Singer, S. M., Zainelli, G. M., Norlund, M. A., Lee, J. M., and Muma, N. A.

(2002) *Neurochem. Int.* **40,** 17–30
80. Oosawa, F., and Asakura, S. (1975) *Thermodynamics of the Polymerization of Protein*, Academic Press, New York
81. Kriem, B., Sponne, I., Fifre, A., Malaplate-Armand, C., Lozac'h-Pillot, K., Koziel, V., Yen-Potin, F. T., Bihain, B., Oster, T., Olivier, J. L., and Pillot, T. (2005) *FASEB J.* **19,** 85–87
82. Malaplate-Armand, C., Florent-Béchard, S., Youssef, I., Koziel, V., Sponne, I., Kriem, B., Leininger-Muller, B., Olivier, J. L., Oster, T., and Pillot, T. (2006) *Neurobiol Dis.* **23,** 178–189
83. Sanchez-Mejia, R. O., Newman, J. W., Toh, S., Yu, G. Q., Zhou, Y., Halabisky, B., Cissé, M., Scearce-Levie, K., Cheng, I. H., Gan, L., Palop, J. J., Bonventre, J. V., and Mucke, L. (2008) *Nat. Neurosci.* **11,** 1311–1318
84. Farooqui, A. A., and Horrocks, L. A. (2006) *Neuroscientist* **12,** 245–260
85. Jicha, G. A., Bowser, R., Kazam, I. G., and Davies, P. (1997) *J. Neurosci. Res.* **48,** 128–132
86. Kanaan, N. M., Morfini, G., Lapointe, N. E., Pigino, G., Patterson, K. R., Song, Y., Andreadis, A., Brady, S. T., and Binder, L. I. (2011) *J. Neurosci.*, in press